

# Engineering an Effective Immune Adjuvant by Designed Control of Shape and Crystallinity of Aluminum Oxyhydroxide Nanoparticles

*Bingbing Sun,<sup>†,1</sup> Zhaoxia Ji,<sup>‡,1</sup> Yu-Pei Liao,<sup>†</sup> Meiyang Wang,<sup>†</sup> Xiang Wang,<sup>†</sup> Juyao Dong,<sup>#</sup>  
Chong Hyun Chang,<sup>‡</sup> Ruibin Li,<sup>†</sup> Haiyuan Zhang,<sup>†</sup> André E. Nel,<sup>†,‡,\*</sup> and Tian Xia<sup>†,‡,\*</sup>*

<sup>†</sup>Division of NanoMedicine, Department of Medicine; <sup>‡</sup>California NanoSystems Institute;

<sup>#</sup>Department of Chemistry, University of California, Los Angeles, CA 90095, United States.

1. Equal contribution

\*Address correspondence to [txia@ucla.edu](mailto:txia@ucla.edu) or [anel@mednet.ucla.edu](mailto:anel@mednet.ucla.edu).

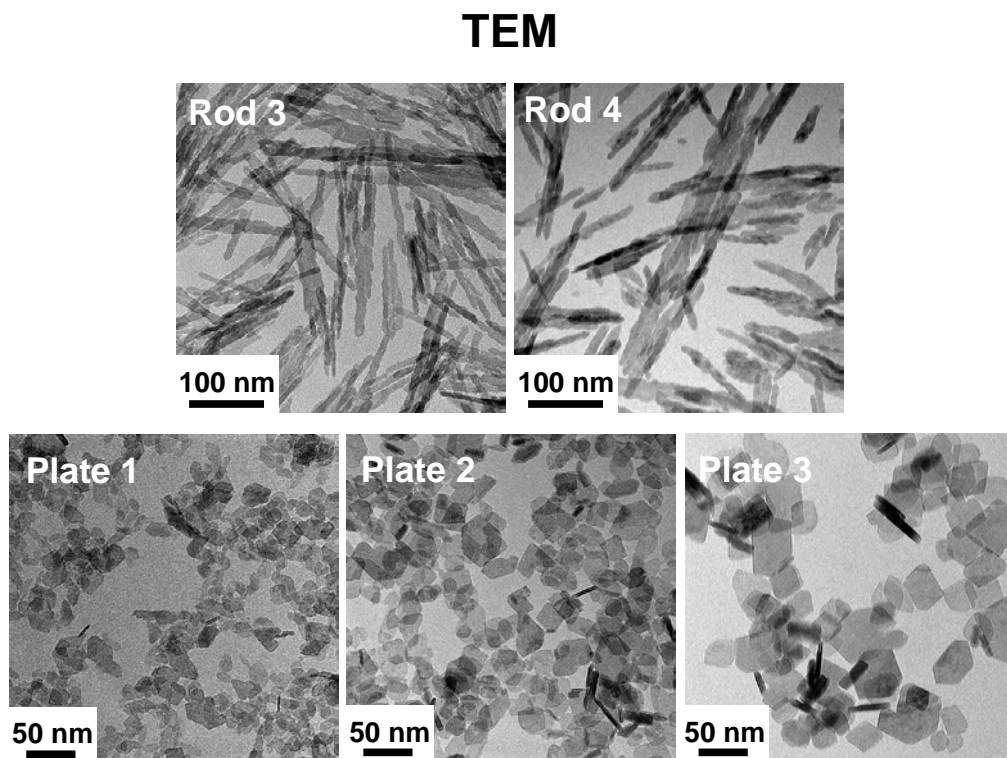
## Supplementary Tables and Figures

Table S1 Blood Serum Biochemistry (average  $\pm$ SD, n=3)<sup>a</sup>

	Normal Range	Ctrl	OVA	Alum+OVA	Rod2+OVA	Rod5+OVA
ALT (U/L)	16-200	5.9 $\pm$ 6.1	10.8 $\pm$ 5.2	12.5 $\pm$ 1.4	8.9 $\pm$ 5.4	12.0 $\pm$ 2.6
AST (U/L)	46-221	89.8 $\pm$ 34.7	148.9 $\pm$ 71.3	120.6 $\pm$ 19.3	117.9 $\pm$ 48.0	69.8 $\pm$ 15.5
BUN (mg/dL)	2-71	18.7 $\pm$ 4.7	20.7 $\pm$ 2.3	22.3 $\pm$ 1.5	18.7 $\pm$ 2.5	25.7 $\pm$ 4.9
CREAT (mg/dL)	0.1-1.8	0.1 $\pm$ 0.0	0.1 $\pm$ 0.0	0.2 $\pm$ 0.0	0.2 $\pm$ 0.0	0.2 $\pm$ 0.0
DBILI (mg/dL)	N/A	0.3 $\pm$ 0.2	0.8 $\pm$ 0.3	0.2 $\pm$ 0.0*	0.3 $\pm$ 0.3	0.4 $\pm$ 0.3
TBILI (mg/dL)	N/A	0.3 $\pm$ 0.2	0.7 $\pm$ 0.1	0.2 $\pm$ 0.0	0.3 $\pm$ 0.1	0.3 $\pm$ 0.2
TP (g/dL)	4.6-7.3	4.8 $\pm$ 0.3	4.9 $\pm$ 0.3	4.4 $\pm$ 0.1	4.6 $\pm$ 0.1	3.5 $\pm$ 1.4

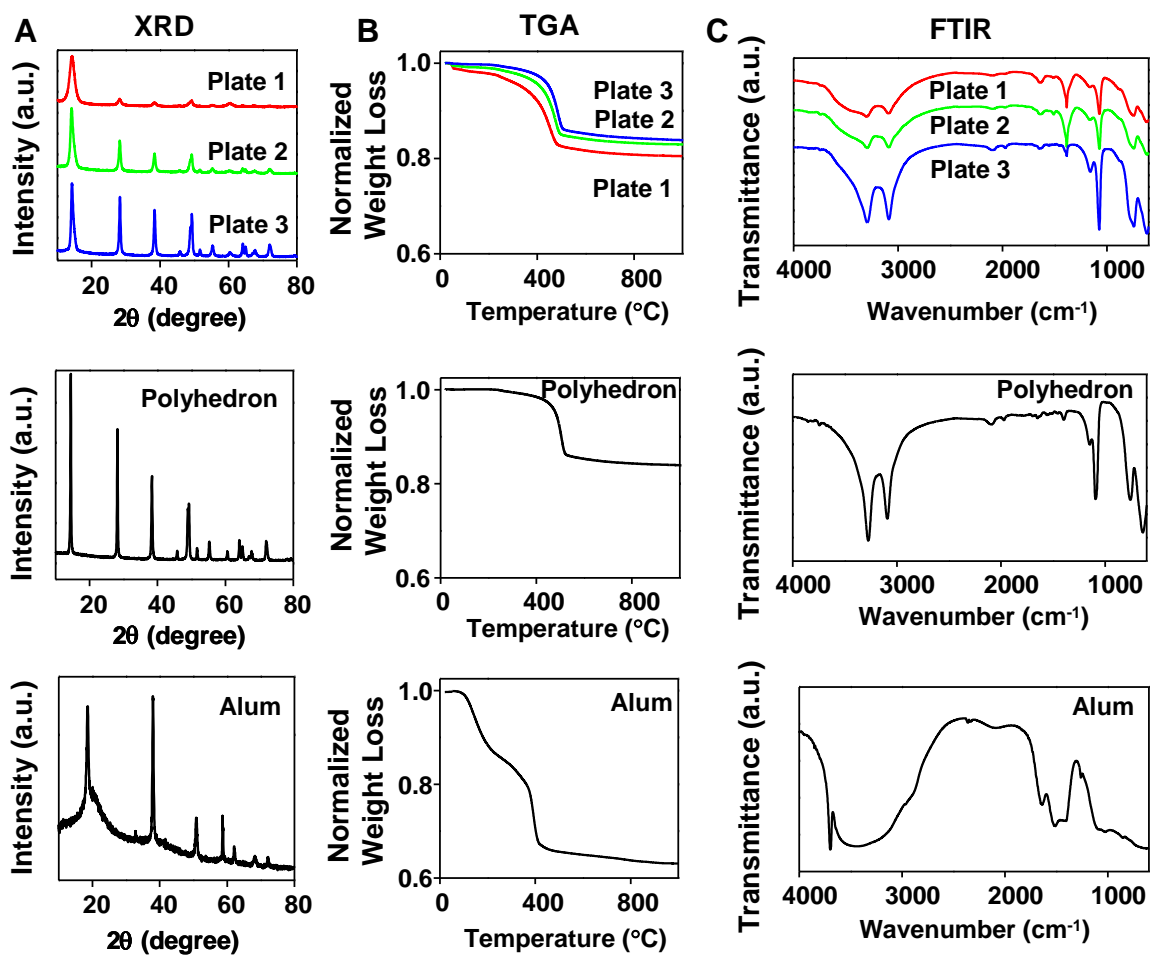
<sup>a</sup>Biochemical parameters includes alanine aminotransferase (ALT), aspartate aminotransferase (AST), blood urea nitrogen (BUN), creatinine (CREAT), direct bilirubin (DBILI), total bilirubin (TBILI), and total protein (TPROT). \*p<0.05 compared with control group.

**Figure S1. TEM analysis of AlOOH nanoparticles.**



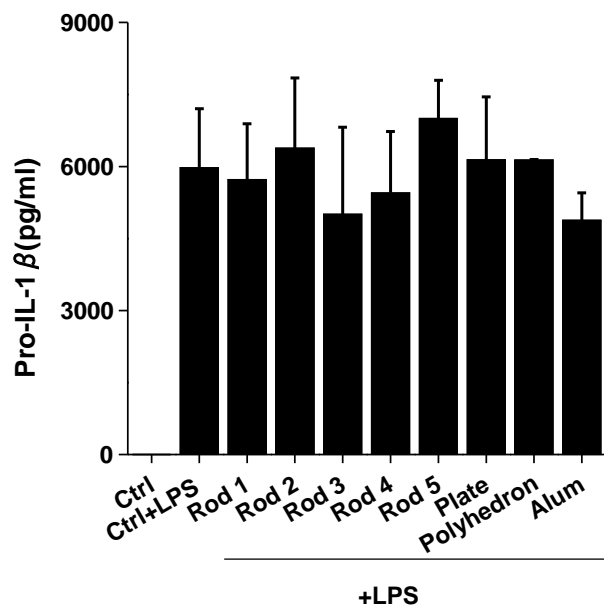
Representative TEM images of AlOOH nanorods obtained using synthesis times of 4 h (Rod 3) and 6 h (Rod 4) as described in materials and methods. The corresponding synthesis times for the nanoplates were 2 h (Plate 1), 4 h (Plate 2), and 24 h (Plate 3). All synthesis reactions were carried out at 200 °C. The images were taken with a JEOL 1200 EX TEM with an accelerating voltage of 80 kV.

Figure S2. Characterization of AlOOH nanoplates, AlOOH nanopolyhedra, and Alum.



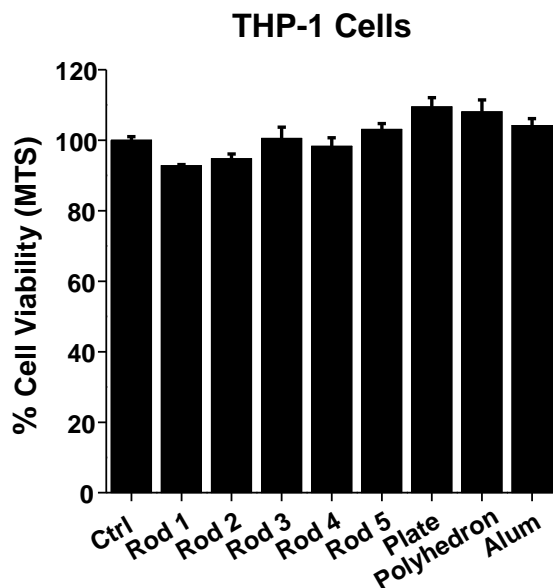
(A) XRD patterns, (B) TGA analysis, and (C) FTIR spectra of AlOOH nanoplates, AlOOH nanopolyhedra and Alum.

**Figure S3. Intracellular pro-IL-1 $\beta$  levels induced by AlOOH nanoparticles in THP-1 cells.**



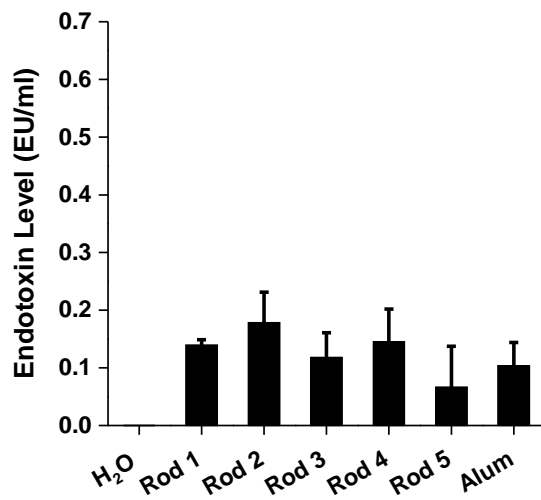
THP-1 cells were exposed to 500  $\mu$ g/ml of AlOOH nanoparticles with LPS (10 ng/ml) for 6 h. Alum was used as a control. Intracellular pro-IL-1 $\beta$  levels were quantified by ELISA (R&D Systems, Minneapolis, MN). Statistical significance was determined by one-way ANOVA.

**Figure S4. Cell viability analysis of AlOOH nanoparticles to THP-1 cells.**



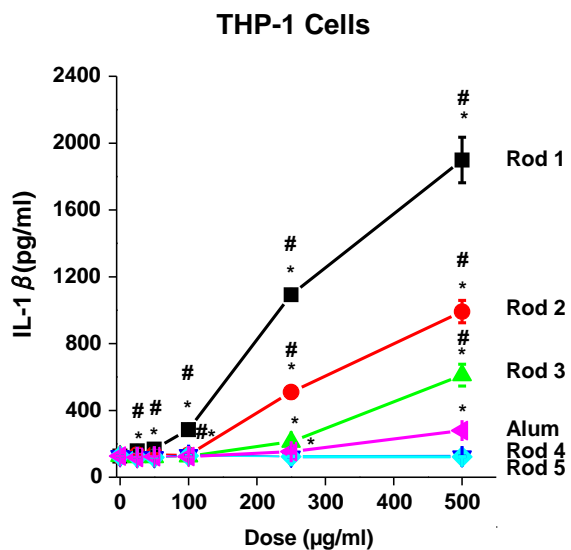
Cell viability of THP-1 cells after exposure to AlOOH nanoparticles was determined using a MTS assay. The cell viability of the nanoparticle-treated cells was normalized according to the value of non-treated control cells, for which the vitality was regarded as 100%.

**Figure S5. Endotoxin levels of AlOOH nanorods.**



The endotoxin levels in 25  $\mu\text{g}$  of AlOOH nanorods (resuspended at 250  $\mu\text{g}/\text{ml}$ ) were determined using a Limulus Amebocyte Lysate assay kit (Lonza, Walkersville, MD).

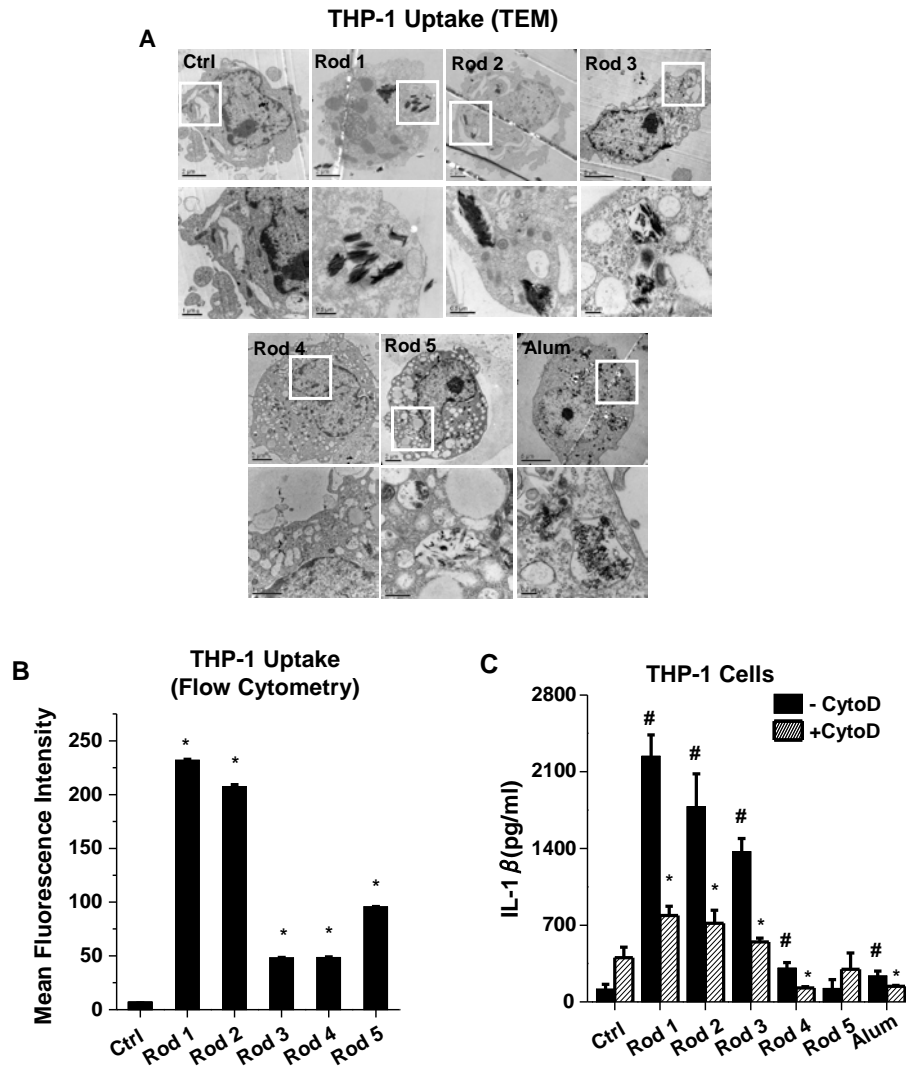
**Figure S6. Dose-dependent IL-1 $\beta$  production induced by AlOOH nanorods in THP-1 cells.**



THP-1 cells were exposed to a wide dose range (25  $\mu\text{g/ml}$  to 500  $\mu\text{g/ml}$ ) of AlOOH nanorods for 6 h. Alum was used as a control. IL-1 $\beta$  production induced by AlOOH nanoparticles was quantified by ELISA. \*  $p < 0.05$  compared to control; #  $p < 0.05$  compared to Alum.

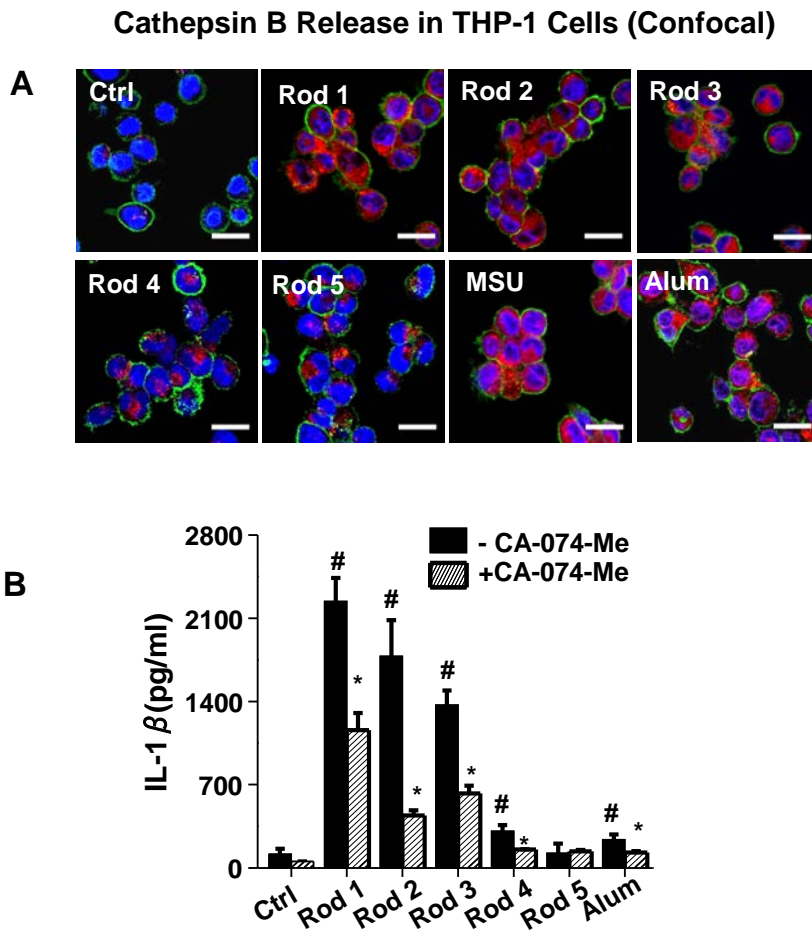


**Figure S7. Cellular uptake and subcellular localization of AIOOH nanorods in THP-1 cells.**



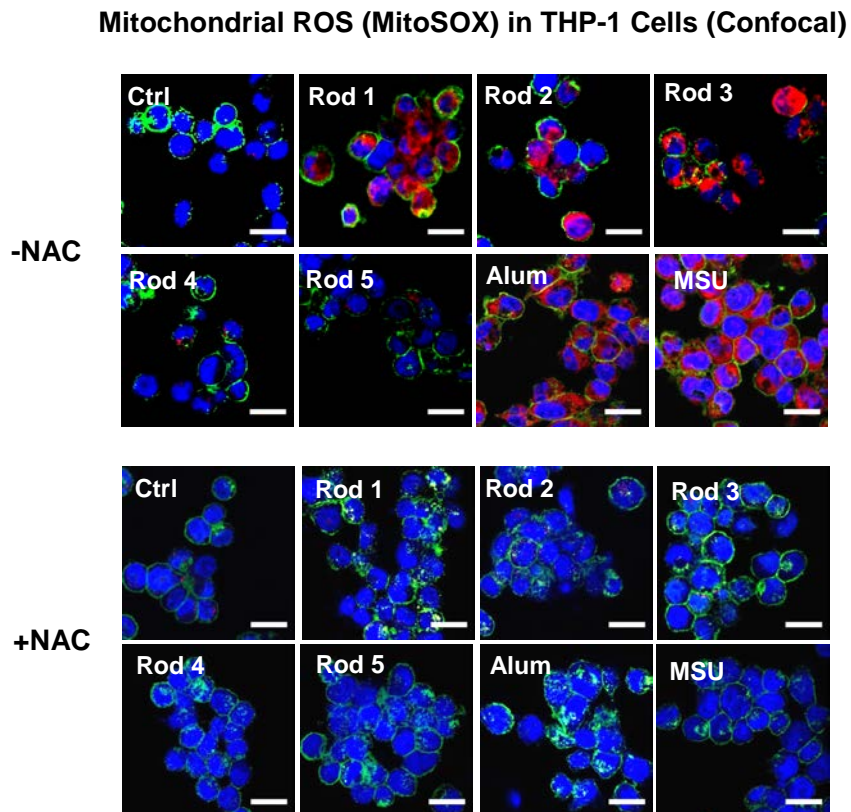
(A) Cellular uptake of nanorods was determined by TEM analysis of THP-1 cells exposed to AIOOH nanorods for 24 h. The images were taken with a JEOL 1200EX electron microscope at 80 kV. (B) Flow cytometry analysis of AIOOH nanorod associated with THP-1 cells. FITC-labeled AIOOH nanorods were exposed to THP-1 cells for 6 h, then the cells were collected for flow cytometry analysis. \*  $p < 0.05$  compared to control. (C) THP-1 cells were pre-treated with 5  $\mu\text{M}$  of cytochalasin D (Cyto D) for 30 min and then the cells were exposed to AIOOH nanorods for an additional 6 h. IL-1 $\beta$  content in the supernatant was quantified by ELISA. \*  $p < 0.05$  compared to THP-1 cells without CytoD treatment; #  $p < 0.05$  compared to control.

**Figure S8. Lysosomal damage and cathepsin B release induced by AIOOH nanorods in THP-1 cells.**



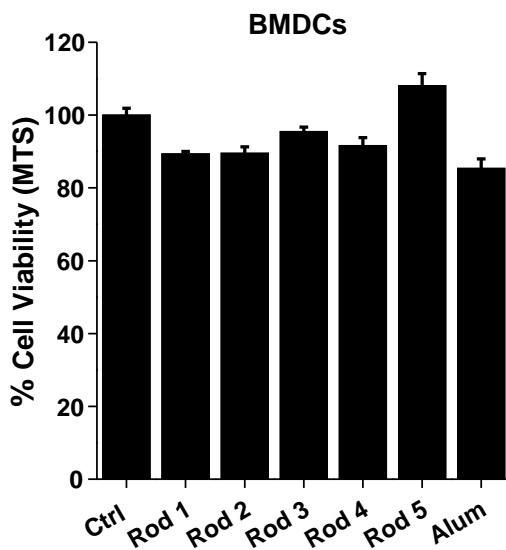
(A) Lysosomal damage and cathepsin B release was determined by confocal microscopy, using a Magic Red-labeled cathepsin B substrate. THP-1 cells were seeded into a 8-well chamber slide and exposed to AIOOH nanorods for 5 h. Cells were stained with Magic Red-labeled cathepsin B substrate for 1 h. Alum and monosodium urate (MSU) crystals were used as controls. The scale bar is 20  $\mu$ m. (B) The effect of the cathepsin B inhibitor, CA-074-Me, on IL-1 $\beta$  production. THP-1 cells were pre-treated with 20  $\mu$ M of inhibitor for 30 min and then exposed to AIOOH nanorods for 6 h. IL-1 $\beta$  release in the supernatant was quantified by ELISA. \* $p$ <0.05 compared to THP-1 cells without CA-074-Me treatment; # $p$ <0.05 compared to control.

**Figure S9. AlOOH nanorods induce ROS generation in THP-1 cells.**



Determination of mitochondrial ROS production in MitoSOX stained cells. After AlOOH nanorod exposure, the cells were stained with 5  $\mu$ M of MitoSOX for 20 min. In order to determine whether this response can be suppressed by an antioxidant, THP-1 cells were pre-treated with 25 mM of NAC for 30 min before nanorod exposure. Alum and monosodium urate (MSU) crystals were used as controls. The scale bar represents 20  $\mu$ m.

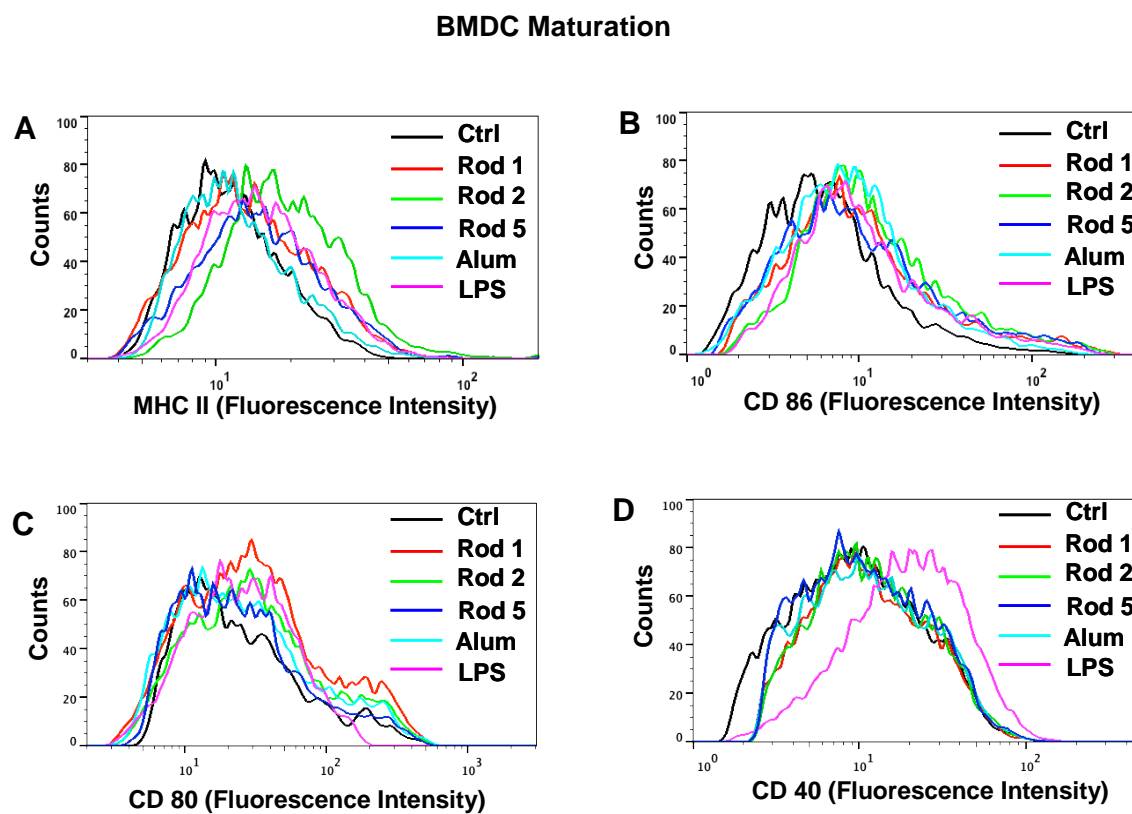
**Figure S10. Cell viability analysis of AlOOH nanorods to BMDCs.**



Cell viability in BMDCs after exposure to AlOOH nanorods was determined using a MTS assay.

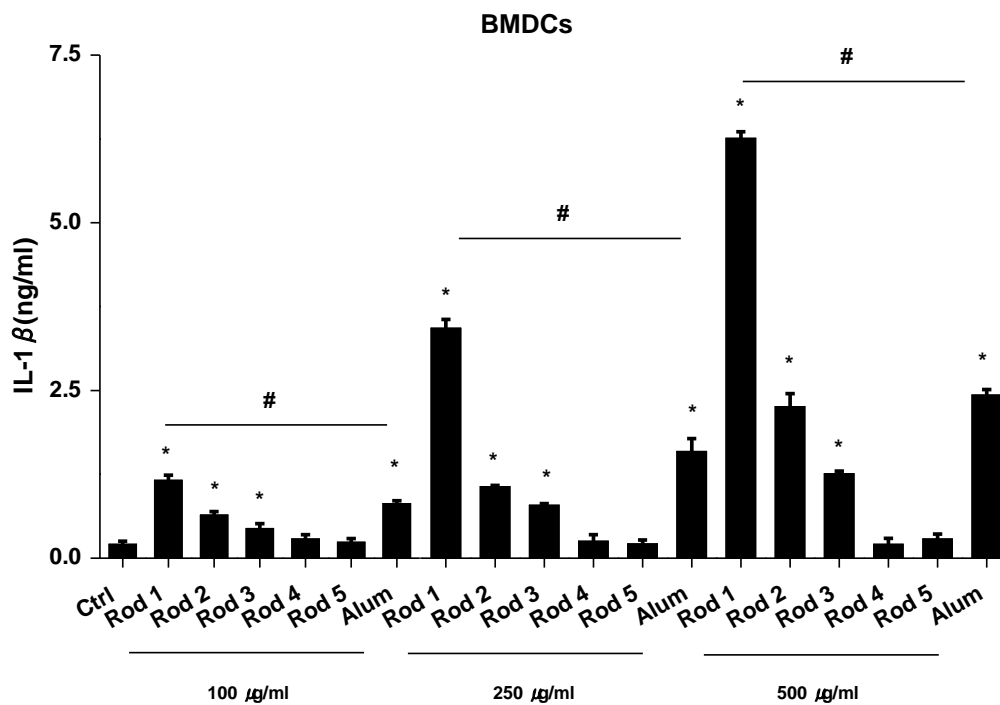
The cell viability of AlOOH nanorod-treated BMDCs was normalized according to the value of control cells, for which the vitality was assumed to be 100%.

**Figure S11. Quantitative measurement of mouse bone marrow-derived dendritic cell (BMDC) maturation.**



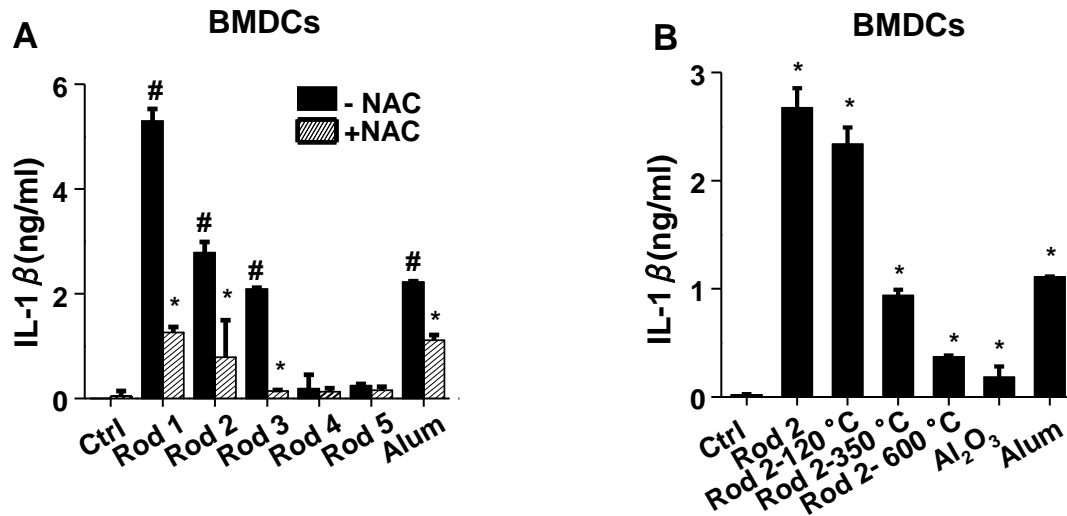
BMDCs were exposed to AlOOH nanorods for 8 h. Surface membrane expression of (A) MHC-II, (B) CD86, (C) CD80 and (D) CD40 on CD11c<sup>+</sup> cells was determined by flow cytometry. LPS-treated (10 ng/ml) BMDCs were used as a control.

**Figure S12. Dose-dependent IL-1 $\beta$  production induced by AlOOH nanorods in BMDCs.**



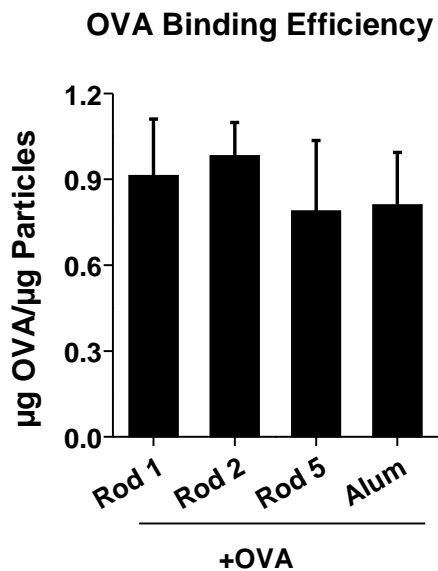
BMDCs were exposed to a wide dose range (100  $\mu\text{g/ml}$  to 500  $\mu\text{g/ml}$ ) of AlOOH nanorods for 6 h. Cells exposed to Alum were used as a control. IL-1 $\beta$  production in response to the nanoparticles was quantified by ELISA. \*  $p < 0.05$  compared to control; #  $p < 0.05$  compared to Alum.

**Figure S13. AlOOH nanorods induce IL-1 $\beta$  production that can be restored by NAC and calcination in BMDCs.**



(A) BMDCs were pre-treated with 25 mM of NAC for 30 min and then were exposed to AlOOH nanorods for 6 h. IL-1 $\beta$  release to the supernatant was determined by ELISA. \* $p < 0.05$  compared to BMDCs without NAC treatment; # $p < 0.05$  compared to control. (B) IL-1 $\beta$  production in BMDCs induced by Rod 2 after thermal treatment at the indicated temperature. \* $p < 0.05$  compared to control.

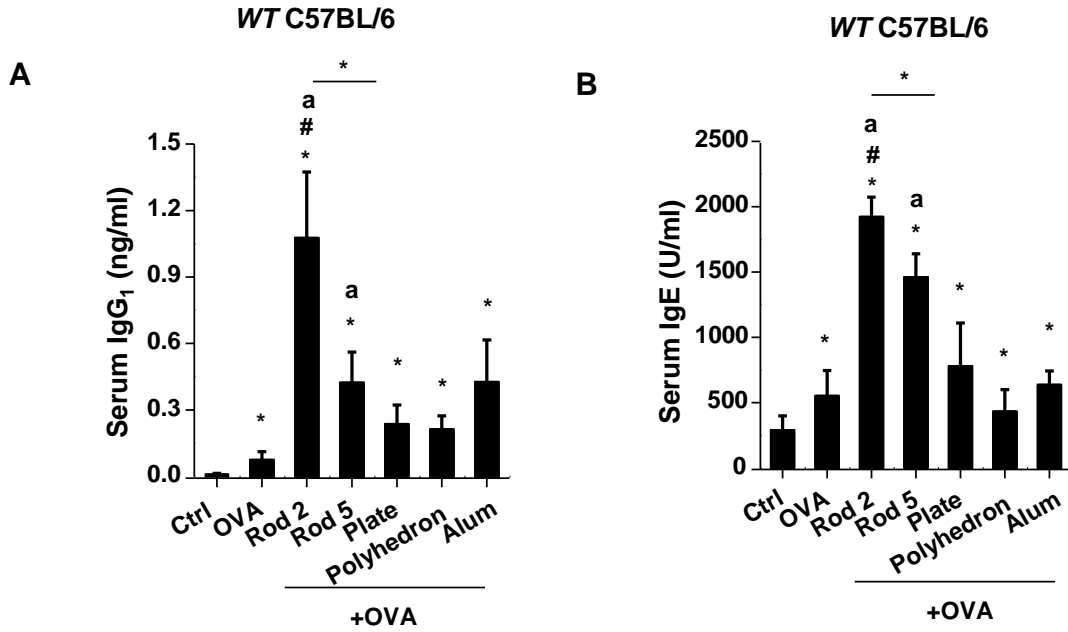
**Figure S14. OVA binding efficiency to AlOOH nanorods.**



100 µl of AlOOH nanorods (100 µg/ml in PBS) was mixed with 100 µl of OVA (100 µg/ml in PBS), and the mixture was incubated for 30 min at room temperature. The particles were centrifuged and the supernatant was collected to analyze the OVA concentration with a BCA protein assay.



**Figure S15. Adjuvant effect of AlOOH nanorods, nanoplates, and nanopolyhedra on humoral immune responses in mice.**



Eight week old female *wt* C57BL/6 mice (6 animals per group) were treated with endotoxin-free OVA (400  $\mu$ g) or OVA/AlOOH nanorods/nanoplates/nanopolyhedra (400  $\mu$ g/2mg) *via i.p.* on day 0. OVA/Alum immunized mice were used as a control. On day 7, the animals were treated with endotoxin-free OVA (200  $\mu$ g) *via i.p.* injection. On day 14, the blood serum was collected to determine (A) IgG<sub>1</sub> and (B) IgE titers in *wt* C57BL/6. \*  $p < 0.05$  compared to control mice; <sup>a</sup> $p < 0.05$  compared to OVA-treated mice; #  $p < 0.05$  compared to OVA/Alum-treated mice.